Bounding Integrity Risk Subject to Structured Time Correlation Modeling Uncertainty

S. Langel, S. Khanafseh, B. Pervan
Illinois Institute of Technology
10 West 32nd Street
Chicago IL, 60616 USA

Abstract—**Sequential state estimation of linear dynamical systems with time correlation uncertainty in the measurement and process noise is considered. The presence of random noise introduces a state estimate error that is defined in terms of a probability distribution. For high integrity navigation applications, the probability of the estimate error vector residing outside a specified boundary must be explicitly quantified. This probability, or integrity risk, can only be computed accurately when the measurement and process noise distributions are precisely known. Unfortunately, precise knowledge of the input noise distributions is rarely available; the use of inexact models can lead to optimistic integrity risks and potentially life-threatening situations can ensue. This paper focuses on developing a methodology to compute upper bounds on integrity risk subject to a bounded uncertainty structure on the input noise autocorrelation functions.**

Keywords- integrity risk; bounded autocorrelation ; Kalman Filter

I. INTRODUCTION

For applications where the unknown state evolves according to a dynamic model, measurements are typically processed (or filtered) over time. In aviation applications, GPS and inertial measurement errors are time-correlated, which must be properly accounted for in the estimation algorithm. State augmentation is the most commonly used approach where filter states are added based on our knowledge of the sensor error autocorrelation function. Since the true mathematical nature of these functions is rarely available, approximate, reduced order models are often employed. For high integrity aviation applications like the Navy's Unmanned Combat Air System (N-UCAS) or Autonomous Airborne Refueling (AAR), it is absolutely essential to determine how these approximate models affect the computed integrity risk.

In the GPS community, an abundance of research has addressed the issue of uncertainty in characterizing the measurement noise. For example, [1] and [2] show how to compute a conservative integrity risk using the concept of cumulative distribution function (CDF) overbounding. These results apply for independent measurement noise; a reasonable assumption for snapshot positioning algorithms. However, this assumption is not appropriate for applications involving measurement filtering due to the presence of time-correlated errors such as multipath.

When the measurement noise also contains an uncertain correlation structure, the problem of ensuring integrity becomes especially difficult. In [3] and [4], the concept of spherical symmetry is used as the framework for treating correlated measurement errors. The symmetric overbounding theorem, stated in [3] and independently verified in [4] provides the necessary theoretical foundation for ensuring integrity in the presence of correlated measurement noise.

Others have taken a more practical approach by considering specialized cases of time correlation uncertainty. For example, [5] considers state estimation using a Kalman filter where the measurement noise is governed by a 1st order Gauss-Markov process. The variance of the process is known, but the time constant is only known to lie within a given interval. Because the Kalman filter is a recursive estimator, it is difficult to account for the impact of previous measurement noise samples on the current state estimate error. In order to account for this in the integrity risk computation, the authors in [5] propose a solution in terms of a bank of Kalman filters. The same estimation problem with Markov noise was considered in [6] using batch weighted least squares estimation. The main conclusion of their work is that integrity risk can be maximized by solving a polynomial root finding problem.

In this work, we use ideas set forth in [3] to provide a new derivation of the Kalman filter estimate error which allows the results provided in [6] to be applied to recursive estimators. We consider the more general problem where the measurement and process noise autocorrelation functions are only known to lie between two known mathematical functions. Given this uncertainty structure, an upper bound on the integrity risk is computed by appropriately selecting the maximum or minimum bounding value for the autocorrelation functions. The algorithms and methods developed in this paper are applied to a one-dimensional, integrated GPS/INS problem.

II. FUNDAMENTAL CONCEPTS

Fault-free integrity risk is defined in this paper as the probability of a scalar linear combination of the estimate error vector residing outside a specified interval.

$$I_{0,\omega} = P\left(\varepsilon_\omega \notin [-a_\omega\ ,\ a_\omega]\right) \tag{1}$$

where $I_{0,\omega}$ is the fault-free integrity risk and ε_ω is defined as

$$\varepsilon_\omega = \hat{\omega} - \omega \tag{2}$$

where $\hat{\omega}$ is an estimate of ω.

In aviation, ω usually indicates a component of the relative position vector and a_ω is the corresponding alert limit. Assuming that ε_ω is a zero-mean Gaussian random variable, $I_{0,\omega}$ can readily be expressed in the form

$$I_{0,\omega} = \operatorname{erfc}\left(\frac{a_\omega}{\sqrt{2\sigma_\omega^2}} \right) \tag{3}$$

where erfc($\bullet$) is the complementary error function and σ_ω^2 is the variance of ε_ω. Since the error function is a monotonically decreasing function, an upper bound on $I_{0,\omega}$ is equivalent to an upper bound on σ_ω^2. This equivalence will be used repeatedly throughout the paper.

To illustrate how σ_ω^2 is obtained, consider the weighted least squares (WLS) estimator for the linear measurement model

$$z = \mathbf{H}_\theta \boldsymbol{\theta} + \mathbf{J}_\nu \boldsymbol{\nu} \tag{4}$$

where z is the measurement vector, $\mathbf{H}_\theta$ is the observation matrix, $\boldsymbol{\theta}$ is the state vector, $\mathbf{J}_\nu$ is the measurement noise mapping matrix and $\boldsymbol{\nu}$ is a zero-mean Gaussian random noise vector with covariance matrix $\mathbf{P}_\nu$.

Equation (4) is a batch measurement model, which means that $\boldsymbol{\nu}$ corresponds to a time series of the measurement error. Therefore, in general $\mathbf{P}_\nu$ will be a fully populated matrix with diagonal elements that capture the noise variance and off-diagonal elements that capture the time correlation present in the measurement noise. Because the precise nature of the time correlation is unknown, an approximate matrix $\hat{\mathbf{P}}_\nu$ is used in the WLS estimator. Given these facts, the estimate error vector is

$$\boldsymbol{\varepsilon}_\theta = \hat{\boldsymbol{\theta}} - \boldsymbol{\theta} = \hat{\mathbf{S}} \mathbf{J}_\nu \boldsymbol{\nu} \tag{5}$$

where $\hat{\mathbf{S}}$ is the weighted left pseudo-inverse of $\mathbf{H}_\theta$ with weighting matrix $\mathbf{W} = \mathbf{J} \hat{\mathbf{P}}_\nu \mathbf{J}^T$.

With ε_ω defined as $\varepsilon_\omega = \boldsymbol{\alpha}_\omega^T \boldsymbol{\varepsilon}_\theta$, where $\boldsymbol{\alpha}_\omega$ is a known vector, we can conclude from (5) that

$$\varepsilon_\omega = \boldsymbol{\alpha}_\omega^T \hat{\mathbf{S}} \mathbf{J}_\nu \boldsymbol{\nu} \tag{6}$$

Evaluating the expected value of ε_ω^2 produces the estimate error variance, σ_ω^2. It was shown in [6] that σ_ω^2 can be expressed directly in terms of the elements of $\mathbf{P}_\nu$.

$$\sigma_\omega^2 = \sum_{ij} \left[\left(\mathbf{J}_\nu^T \hat{\mathbf{S}}^T \boldsymbol{\alpha}_\omega \boldsymbol{\alpha}_\omega^T \hat{\mathbf{S}} \mathbf{J}_\nu \right) \circ \mathbf{P}_\nu \right]_{ij} \tag{7}$$

where the symbol $\circ$ is used to indicate the entry-wise product of two matrices [9].

The elements of $\mathbf{P}_\nu$ are values of the measurement noise autocorrelation function. In this work, these values are constrained to lie between two known mathematical functions, as shown in Fig. 1.

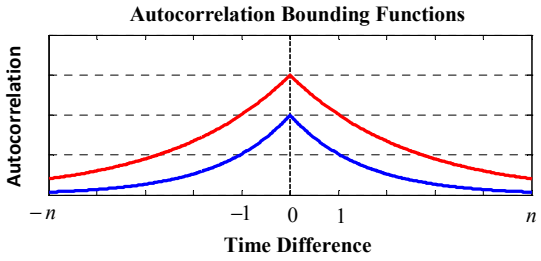

Figure 1. Exponential autocorrelation bounding functions

It was assumed in [6] that the measurement noise is governed by a 1st order Gauss-Markov process. Under this assumption, σ_ω^2 was maximized subject to the uncertainty structure shown in Fig. 1 via polynomial root finding. Of course, it is very difficult to very that the measurement noise is *exactly* 1st order Gauss-Markov. A more natural state of knowledge is that the autocorrelation function is only known to lie between the two bounding functions, without any specific knowledge of its mathematical form. In this case, it is possible to upper bound σ_ω^2 directly by appropriately choosing the values of the upper and lower bounding functions. To see this, consider the following form for $\mathbf{P}_\nu$.

$$\mathbf{P}_\nu = \begin{bmatrix} r_0 & r_1 & r_2 & \cdots & r_n \\ r_1 & r_0 & r_1 & \ddots & \vdots \\ r_2 & r_1 & \ddots & \ddots & r_2 \\ \vdots & \ddots & \ddots & r_0 & r_1 \\ r_n & \cdots & r_2 & r_1 & r_0 \end{bmatrix} \tag{8}$$

where r_k is the value of the autocorrelation function at a time shift of k.

Making the definition $\mathbf{D} = \mathbf{J}_\nu^T \hat{\mathbf{S}}^T \boldsymbol{\alpha}_\omega \boldsymbol{\alpha}_\omega^T \hat{\mathbf{S}} \mathbf{J}_\nu$ and using the definition of the entry-wise product, (7) can be written as

$$\sigma_\omega^2 = c_0 r_0 + 2\sum_{i=1}^{n} c_i r_i \tag{9}$$

where c_i is the sum of the elements along the i^{th} diagonal of the matrix, **D**.

Now, in order to determine an upper bound on σ_ω^2, we only need to consider the sign of the c_i's. That is, if c_i is a positive number, then we assign the value of the upper bounding function to r_i. If c_i is a negative number, then we assign the value of the lower bounding function to r_i.

Notice that when using batch WLS estimation it is straightforward to describe how the entire original measurement noise sequence affects the estimate error, as shown in (6). However, batch estimation techniques are inefficient for dynamical systems with large data records. The Kalman filter is a recursive optimal estimator that performs well in these situations, but requires specific mathematical models to describe the time correlation in the measurement and process noise. As a result, the modeling uncertainty is transferred to the matrices describing the state dynamic model. At first glance it appears that an equation similar to (6) cannot be obtained for the Kalman filter, given its recursive nature and the need for state augmentation. In the next section, we will see how this is possible by deriving an alternative expression for the Kalman state estimate error vector.

III. Fundamentals of Kalman Filtering

At any instant *k*, the measurement model shown in (4) can be written as

$$\boldsymbol{z}_k = \mathbf{H}_{\theta,k}\boldsymbol{\theta}_k + \mathbf{J}_{\nu,k}\boldsymbol{\nu}_k \tag{10}$$

In general, $\boldsymbol{\theta}_k$ evolves in time according to the dynamic model

$$\boldsymbol{\theta}_{k+1} = \mathbf{F}_{\theta,k}\boldsymbol{\theta}_k + \mathbf{G}_{\theta,k}\boldsymbol{w}_k \tag{11}$$

where $\mathbf{F}_{\theta,k}$ is the state transition matrix, $\mathbf{G}_{\theta,k}$ is the process noise mapping matrix and $\boldsymbol{w}_k$ is the process noise vector.

The discrete-time Kalman filter is the maximum likelihood estimator for the linear models shown in (10) and (11) provided that $\boldsymbol{\nu}_k$ and $\boldsymbol{w}_k$ are mutually uncorrelated, zero-mean Gaussian white noise (GWN) processes [7], [8]. In this paper, we will assume that $\boldsymbol{w}_k$ and $\boldsymbol{\nu}_k$ are always uncorrelated. However, individually, they may possess some degree of time correlation and hence need not be white noise processes. In this case, the method of state augmentation can be used to account for time correlation as long as $\boldsymbol{w}_k$ and $\boldsymbol{\nu}_k$ can be written in the form

$$\boldsymbol{w}_k = \mathbf{A}_k\boldsymbol{\xi}_k + \mathbf{B}_k\boldsymbol{q}_{\theta,k} \tag{12}$$

$$\boldsymbol{\nu}_k = \mathbf{C}_k\boldsymbol{\eta}_k + \mathbf{D}_k\boldsymbol{r}_k \tag{13}$$

where $\mathbf{A}_k$, $\mathbf{B}_k$, $\mathbf{C}_k$ and $\mathbf{D}_k$ are known matrices, $\boldsymbol{q}_{\theta,k}$ and $\boldsymbol{r}_k$ are zero-mean GWN processes and $\boldsymbol{\xi}_k$ and $\boldsymbol{\eta}_k$ are Gaussian random processes governed by the following linear equations

$$\boldsymbol{\xi}_{k+1} = \mathbf{F}_{\xi,k}\boldsymbol{\xi}_k + \mathbf{G}_{\xi,k}\boldsymbol{q}_{\xi,k} \tag{14}$$

$$\boldsymbol{\eta}_{k+1} = \mathbf{F}_{\eta,k}\boldsymbol{\eta}_k + \mathbf{G}_{\eta,k}\boldsymbol{q}_{\eta,k} \tag{15}$$

where $\mathbf{F}_{\xi,k}$, $\mathbf{G}_{\xi,k}$, $\mathbf{F}_{\eta,k}$ and $\mathbf{G}_{\eta,k}$ are known matrices and $\boldsymbol{q}_{\xi,k}$ and $\boldsymbol{q}_{\eta,k}$ are zero-mean GWN processes.

Inserting (12) and (13) into (10) and (11) yields

$$\boldsymbol{z}_k = \mathbf{H}_{\theta,k}\boldsymbol{\theta}_k + \mathbf{J}_{\nu,k}(\mathbf{C}_k\boldsymbol{\eta}_k + \mathbf{D}_k\boldsymbol{r}_k) \tag{16}$$

$$\boldsymbol{\theta}_{k+1} = \mathbf{F}_{\theta,k}\boldsymbol{\theta}_k + \mathbf{G}_{\theta,k}(\mathbf{A}_k\boldsymbol{\xi}_k + \mathbf{B}_k\boldsymbol{q}_{\theta,k}) \tag{17}$$

Equations (14) through (17) can be written in the augmented form

$$\boldsymbol{z}_k = \begin{bmatrix}\mathbf{H}_{\theta,k} & \mathbf{0} & \mathbf{J}_{\nu,k}\mathbf{C}_k\end{bmatrix}\begin{bmatrix}\boldsymbol{\theta}_k\\ \boldsymbol{\xi}_k\\ \boldsymbol{\eta}_k\end{bmatrix} + \mathbf{J}_{\nu,k}\mathbf{D}_k\boldsymbol{r}_k \tag{18}$$

$$\begin{bmatrix}\boldsymbol{\theta}_{k+1}\\ \boldsymbol{\xi}_{k+1}\\ \boldsymbol{\eta}_{k+1}\end{bmatrix} = \begin{bmatrix}\mathbf{F}_{\theta,k} & \mathbf{G}_{\theta,k}\mathbf{A}_k & \mathbf{0}\\ \mathbf{0} & \mathbf{F}_{\xi,k} & \mathbf{0}\\ \mathbf{0} & \mathbf{0} & \mathbf{F}_{\eta,k}\end{bmatrix}\begin{bmatrix}\boldsymbol{\theta}_k\\ \boldsymbol{\xi}_k\\ \boldsymbol{\eta}_k\end{bmatrix} + \begin{bmatrix}\mathbf{G}_{\theta,k}\mathbf{B}_k & \mathbf{0} & \mathbf{0}\\ \mathbf{0} & \mathbf{G}_{\xi,k} & \mathbf{0}\\ \mathbf{0} & \mathbf{0} & \mathbf{G}_{\eta,k}\end{bmatrix}\begin{bmatrix}\boldsymbol{q}_{\theta,k}\\ \boldsymbol{q}_{\xi,k}\\ \boldsymbol{q}_{\eta,k}\end{bmatrix} \tag{19}$$

which can also be expressed more compactly as

$$\boldsymbol{z}_k = \mathbf{H}_k\boldsymbol{x}_k + \mathbf{J}_k\boldsymbol{r}_k \tag{20}$$

$$\boldsymbol{x}_{k+1} = \mathbf{F}_k\boldsymbol{x}_k + \mathbf{G}_k\boldsymbol{q}_k \tag{21}$$

The fact that $\boldsymbol{q}_{\theta,k}$, $\boldsymbol{q}_{\xi,k}$ and $\boldsymbol{q}_{\eta,k}$ are white noise processes does not necessarily imply that $\boldsymbol{q}_k$ is a white noise process. Despite this difficulty, it will be assumed that the noise decomposition given in (12) through (15) is performed such that $\boldsymbol{q}_k$ and $\boldsymbol{r}_k$ are mutually uncorrelated, zero-mean GWN processes. Therefore, (20) and (21) describe an estimation problem amenable to a Kalman filtering solution.

TABLE I. DISCRETE-TIME KALMAN FILTER

Measurement Update	Time Update
$\mathbf{K}_k = \mathbf{P}_k^- \mathbf{H}_k^T \left(\mathbf{H}_k \mathbf{P}_k^- \mathbf{H}_k^T + \mathbf{J}_k \mathbf{R}_k \mathbf{J}_k^T \right)$	
$\hat{\boldsymbol{x}}_k = \hat{\boldsymbol{x}}_k^- + \mathbf{K}_k \left(z_k - \mathbf{H}_k \hat{\boldsymbol{x}}_k^- \right)$	$\hat{\boldsymbol{x}}_{k+1}^- = \mathbf{F}_k \hat{\boldsymbol{x}}_k$
$\mathbf{P}_k = (\mathbf{I} - \mathbf{K}_k \mathbf{H}_k) \mathbf{P}_k^-$	$\mathbf{P}_{k+1}^- = \mathbf{F}_k \mathbf{P}_k \mathbf{F}_k^T + \mathbf{G}_k \mathbf{Q}_k \mathbf{G}_k^T$

The initial state $\boldsymbol{x}_0$ is assumed to be a Gaussian random vector with known mean and covariance matrix that are used to initialize the filter.

$$\hat{x}_0^- = E[\boldsymbol{x}_0] \tag{22}$$

$$\hat{\mathbf{P}}_0^- = E\left\{ \left[x_0 - E[\boldsymbol{x}_0] \right] \left[x_0 - E[\boldsymbol{x}_0] \right]^T \right\} \tag{23}$$

Notice that there are two estimates of the state vector available at time k, namely $\hat{\boldsymbol{x}}_k^-$ and $\hat{\boldsymbol{x}}_k$, each with an error covariance matrix of $\mathbf{P}_k^-$ and $\mathbf{P}_k$, respectively. It is important to note that the error covariance matrix completely specifies the probability distribution of the state estimate error vector. This is due to the fact that the Kalman filter is a linear unbiased estimator and all noise processes are zero-mean GWN processes. However, $\mathbf{P}_k^-$ and $\mathbf{P}_k$ as computed in table I are only meaningful if $\mathbf{F}_k$, $\mathbf{G}_k$, $\mathbf{H}_k$, $\mathbf{J}_k$, $\mathbf{Q}_k$ and $\mathbf{R}_k$ are precisely known. There is always some uncertainty in specifying these matrices and we will now discuss how to quantify the impact of this uncertainty on the estimate error for the Kalman filter.

IV. KALMAN FILTERING WITH UNCERTAINTY

In (18), the state vector was shown to be

$$\boldsymbol{x}_k = [\boldsymbol{\theta}_k^T \quad \boldsymbol{\xi}_k^T \quad \boldsymbol{\eta}_k^T]^T \tag{24}$$

Recall that $\boldsymbol{\xi}_k$ and $\boldsymbol{\eta}_k$ were added to model the colored nature of the process and measurement noise. Aside from this purpose, there are nuisance states which implies that integrity risk will be computed for linear combinations of $\boldsymbol{\theta}_k$. Remember that our primary goal is to obtain an equation for the Kalman filter that resembles (6). That is, an equation that describes how the original measurement and process noise sequences $\boldsymbol{\nu}_k$ and $\boldsymbol{w}_k$ affect that portion of the estimate error vector corresponding to $\boldsymbol{\theta}_k$. From table I, the state estimate after a measurement update is given by

$$\hat{\boldsymbol{x}}_k = \hat{\boldsymbol{x}}_k^- + \mathbf{K}_k (z_k - \mathbf{H}_k \hat{\boldsymbol{x}}_k^-) \tag{25}$$

Substituting the measurement model from (10) for z_k and the observation matrix from (18) for $\mathbf{H}_k$ and simplifying the result yields

$$\begin{bmatrix} \hat{\boldsymbol{\theta}}_k \\ \hat{\boldsymbol{\xi}}_k \\ \hat{\boldsymbol{\eta}}_k \end{bmatrix} = \begin{bmatrix} \hat{\boldsymbol{\theta}}_k^- \\ \hat{\boldsymbol{\xi}}_k^- \\ \hat{\boldsymbol{\eta}}_k^- \end{bmatrix} - \mathbf{K}_k \left\{ \mathbf{H}_k \begin{bmatrix} \hat{\boldsymbol{\theta}}_k^- - \boldsymbol{\theta}_k \\ \hat{\boldsymbol{\xi}}_k^- \\ \hat{\boldsymbol{\eta}}_k^- \end{bmatrix} - \mathbf{J}_{\nu,k} \boldsymbol{\nu}_k \right\} \tag{26}$$

Now subtract the vector $[\boldsymbol{\theta}_k^T \quad \mathbf{0}^T \quad \mathbf{0}^T]^T$ from both sides of (26).

$$\begin{bmatrix} \hat{\boldsymbol{\theta}}_k - \boldsymbol{\theta}_k \\ \hat{\boldsymbol{\xi}}_k \\ \hat{\boldsymbol{\eta}}_k \end{bmatrix} = \begin{bmatrix} \hat{\boldsymbol{\theta}}_k^- - \boldsymbol{\theta}_k \\ \hat{\boldsymbol{\xi}}_k^- \\ \hat{\boldsymbol{\eta}}_k^- \end{bmatrix} - \mathbf{K}_k \left\{ \mathbf{H}_k \begin{bmatrix} \hat{\boldsymbol{\theta}}_k^- - \boldsymbol{\theta}_k \\ \hat{\boldsymbol{\xi}}_k^- \\ \hat{\boldsymbol{\eta}}_k^- \end{bmatrix} - \mathbf{J}_{\nu,k} \boldsymbol{\nu}_k \right\} \tag{27}$$

Making the definitions

$$\boldsymbol{\varepsilon}_{\theta,k} = \hat{\boldsymbol{\theta}}_k - \boldsymbol{\theta}_k \tag{28}$$

$$\boldsymbol{\varepsilon}_{\theta,k}^- = \hat{\boldsymbol{\theta}}_k^- - \boldsymbol{\theta}_k \tag{29}$$

allows (27) to be written as

$$\begin{bmatrix} \boldsymbol{\varepsilon}_{\theta,k} \\ \hat{\boldsymbol{\xi}}_k \\ \hat{\boldsymbol{\eta}}_k \end{bmatrix} = (\mathbf{I} - \mathbf{K}_k \mathbf{H}_k) \begin{bmatrix} \boldsymbol{\varepsilon}_{\theta,k}^- \\ \hat{\boldsymbol{\xi}}_k^- \\ \hat{\boldsymbol{\eta}}_k^- \end{bmatrix} + \mathbf{K}_k \mathbf{J}_{\nu,k} \boldsymbol{\nu}_k \tag{30}$$

A similar procedure can be followed to determine how $\boldsymbol{w}_k$ affects the estimate error vector. From table I, the state estimate after a time update is given by

$$\begin{bmatrix} \hat{\boldsymbol{\theta}}_{k+1}^- \\ \hat{\boldsymbol{\xi}}_{k+1}^- \\ \hat{\boldsymbol{\eta}}_{k+1}^- \end{bmatrix} = \mathbf{F}_k \begin{bmatrix} \hat{\boldsymbol{\theta}}_k \\ \hat{\boldsymbol{\xi}}_k \\ \hat{\boldsymbol{\eta}}_k \end{bmatrix} \tag{31}$$

Subtracting the vector $[\boldsymbol{\theta}_{k+1}^T \quad \mathbf{0}^T \quad \mathbf{0}^T]^T$ from both sides of (31) yields

$$\begin{bmatrix} \hat{\boldsymbol{\theta}}_{k+1}^- - \boldsymbol{\theta}_{k+1} \\ \hat{\boldsymbol{\xi}}_{k+1}^- \\ \hat{\boldsymbol{\eta}}_{k+1}^- \end{bmatrix} = \mathbf{F}_k \begin{bmatrix} \hat{\boldsymbol{\theta}}_k \\ \hat{\boldsymbol{\xi}}_k \\ \hat{\boldsymbol{\eta}}_k \end{bmatrix} - \begin{bmatrix} \boldsymbol{\theta}_{k+1} \\ \mathbf{0} \\ \mathbf{0} \end{bmatrix} \tag{32}$$

From (19), we know that

$$\begin{bmatrix} \boldsymbol{\theta}_{k+1} \\ \mathbf{0} \\ \mathbf{0} \end{bmatrix} = \mathbf{F}_k \begin{bmatrix} \boldsymbol{\theta}_k \\ \mathbf{0} \\ \mathbf{0} \end{bmatrix} + \begin{bmatrix} \mathbf{G}_{\theta,k} \\ \mathbf{0} \\ \mathbf{0} \end{bmatrix} \boldsymbol{w}_k \tag{33}$$

Substituting (33) into the right hand side of (32) results in

$$\begin{bmatrix} \boldsymbol{\varepsilon}_{\theta,k+1}^- \\ \hat{\boldsymbol{\xi}}_{k+1}^- \\ \hat{\boldsymbol{\eta}}_{k+1}^- \end{bmatrix} = \mathbf{F}_k \begin{bmatrix} \boldsymbol{\varepsilon}_{\theta,k} \\ \hat{\boldsymbol{\xi}}_k \\ \hat{\boldsymbol{\eta}}_k \end{bmatrix} - \begin{bmatrix} \mathbf{G}_{\theta,k} \\ \mathbf{0} \\ \mathbf{0} \end{bmatrix} \boldsymbol{w}_k \tag{34}$$

Making the following definitions

$$\widetilde{\mathbf{A}}_k = \mathbf{F}_k \tag{35}$$

$$\widetilde{\mathbf{B}}_k = \begin{bmatrix} -\mathbf{G}_{\theta,k}^T & \mathbf{0}^T & \mathbf{0}^T \end{bmatrix}^T \tag{36}$$

$$\widetilde{\mathbf{C}}_k = \left(\mathbf{I} - \mathbf{K}_k \mathbf{H}_k \right) \tag{37}$$

$$\widetilde{\mathbf{D}}_k = \mathbf{K}_k \mathbf{J}_{\nu,k} \boldsymbol{\nu}_k \tag{38}$$

$$\widetilde{\boldsymbol{\varepsilon}}_k = \begin{bmatrix} \boldsymbol{\varepsilon}_{\theta,k}^T & \hat{\boldsymbol{\xi}}_k^T & \boldsymbol{\eta}_k^T \end{bmatrix}^T \tag{39}$$

allows (30) and (34) to be written more succinctly as

$$\widetilde{\boldsymbol{\varepsilon}}_k = \widetilde{\mathbf{C}}_k \widetilde{\boldsymbol{\varepsilon}}_k^- + \widetilde{\mathbf{D}}_k \boldsymbol{\nu}_k \tag{40}$$

$$\widetilde{\boldsymbol{\varepsilon}}_{k+1}^- = \widetilde{\mathbf{A}}_{k+1} \widetilde{\boldsymbol{\varepsilon}}_k + \widetilde{\mathbf{B}}_{k+1} \boldsymbol{w}_k \tag{41}$$

Equations (40) and (41) accomplish our initial objective: to find a set of equations that describe how the original measurement and process noise sequences affect that portion of the state estimate error vector critical to integrity. As pointed out in [3], the general solution to (40) and (41) can be expressed in terms of an initial condition response and an impulse response. In the next section, we will present the solution in terms of an algorithm that can easily be implemented.

V. Solution to Linear Difference Equations

In general, measurements will be available from multiple sensors and the dynamic system will be subjected to multiple disturbances, leading to the following definitions for $\boldsymbol{\nu}_k$ and $\boldsymbol{w}_k$.

$$\boldsymbol{\nu}_k = [\, \nu_{1,k} \quad \nu_{2,k} \quad \cdots \quad \nu_{m,k} \,]^T \tag{42}$$

$$\boldsymbol{w}_k = [\, w_{1,k} \quad w_{2,k} \quad \cdots \quad \nu_{p,k} \,]^T \tag{43}$$

With these definitions, the solution to (40) and (41) before and after a measurement update can be written as

$$\widetilde{\boldsymbol{\varepsilon}}_{k+1}^- = \boldsymbol{\Phi}_{k+1}^- \widetilde{\boldsymbol{\varepsilon}}_0^- + \sum_{i=1}^{p} \boldsymbol{\Gamma}_{i,k+1}^- \overline{\boldsymbol{w}}_i + \sum_{i=1}^{m} \boldsymbol{\Lambda}_{i,k+1}^- \overline{\boldsymbol{\nu}}_i \tag{44}$$

$$\widetilde{\boldsymbol{\varepsilon}}_k = \boldsymbol{\Phi}_k \widetilde{\boldsymbol{\varepsilon}}_0^- + \sum_{i=1}^{p} \boldsymbol{\Gamma}_i \boldsymbol{w}_i + \sum_{i=1}^{m} \boldsymbol{\Lambda}_i \boldsymbol{\nu}_i \tag{45}$$

Where wbari is a time series of the process noise from sensor I and vbari is a time series of the measurement noise from sensor i. Each of the matrices is updated as follows

TABLE II. DISCRETE-TIME KALMAN FILTER

Measurement Update	Time Update
$\boldsymbol{\Gamma}_{i,k} = \left[\widetilde{\mathbf{C}}_k \boldsymbol{\Gamma}_{i,k}^- \mid \widetilde{\boldsymbol{d}}_{i,k} \right]$, $i = 1$ to p	$\boldsymbol{\Gamma}_{i,k+1}^- = \widetilde{\mathbf{A}}_{k+1} \boldsymbol{\Gamma}_{i,k}$, $i = 1$ to p
$\boldsymbol{\Phi}_k = \widetilde{\mathbf{C}}_k \boldsymbol{\Phi}_k^-$	$\boldsymbol{\Phi}_{k+1}^- = \widetilde{\mathbf{A}}_{k+1} \boldsymbol{\Phi}_k$
$\boldsymbol{\Lambda}_{i,k} = \widetilde{\mathbf{C}}_k \boldsymbol{\Lambda}_{i,k}^-$, $i = 1$ to m	$\boldsymbol{\Lambda}_{i,k+1} = \left[\widetilde{\mathbf{A}}_{k+1} \boldsymbol{\Lambda}_k \mid \widetilde{\boldsymbol{b}}_{i,k} \right]$, $i = 1$ to m

VI. Numerical Simulation

In order to illustrate the methods described above, consider the problem shown in Fig. 2. The position and velocity of the vehicle along the *x*-axis are estimated using an accelerometer attached to the vehicle and a ranging beacon located at the origin. Assuming that the coordinate system is horizontal and constitutes an inertial reference frame, the measurement and state dynamic models are given by

$$\dot{x} = u \tag{46}$$

$$\dot{u} = f + w \tag{47}$$

$$z_k = x_k + \nu_k \tag{48}$$

where x is the position of the vehicle along the x-axis, u is the velocity of the vehicle along the x-axis, f is the true specific force in the x-direction, w is a random disturbance input and z_k is the ranging measurement at time k with an error of ν_k.

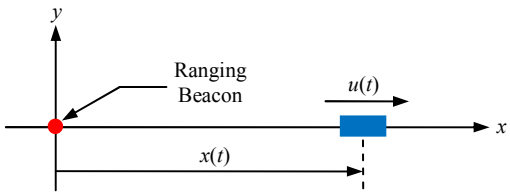

Figure 2. 1–D position and velocity estimation

The measurement and process noise are decomposed as

$$w = \xi + q_u \tag{49}$$

$$\nu_k = \eta_k + r_k \tag{50}$$

where q_u and r_k are mutually uncorrelated, GWN processes and ξ and η_k are *modeled* as

$$\dot{\xi} = -\frac{1}{\tau_\xi}\xi + q_\xi \tag{51}$$

$$\dot{\eta} = -\frac{1}{\tau_\eta}\eta + q_\eta \tag{52}$$

where q_ξ and q_η are mutually uncorrelated, GWN processes that are also uncorrelated with r_k.

When taken together, (46) through (52) define the following estimation problem

$$\begin{bmatrix}\dot{x}\\ \dot{u}\\ \dot{\xi}\\ \dot{\eta}\end{bmatrix} = \begin{bmatrix}0 & 1 & 0 & 0\\ 0 & 0 & 1 & 0\\ 0 & 0 & -\beta_\xi & 0\\ 0 & 0 & 0 & -\beta_\eta\end{bmatrix}\begin{bmatrix}x\\ u\\ \xi\\ \eta\end{bmatrix} + \begin{bmatrix}0\\ 1\\ 0\\ 0\end{bmatrix} f + \begin{bmatrix}0 & 0 & 0\\ 1 & 0 & 0\\ 0 & 1 & 0\\ 0 & 0 & 1\end{bmatrix}\begin{bmatrix}q_u\\ q_\xi\\ q_\eta\end{bmatrix} \tag{53}$$

$$z_k = \begin{bmatrix}1 & 0 & 0 & 1\end{bmatrix}\begin{bmatrix}x_k\\ u_k\\ \xi_k\\ \eta_k\end{bmatrix} + r_k \tag{54}$$

where $\beta_\xi = 1/\tau_\xi$ and $\beta_\eta = 1/\tau_\eta$.

Before we can apply the bounding methods developed earlier, we must convert the continuous-discrete system shown in (53) and (54) entirely to discrete form. In this work, the Van Loan algorithm discussed in [8] is used to complete the conversion.

$$z_k = \mathbf{H}\boldsymbol{x}_k + r_k \tag{55}$$

$$\boldsymbol{x}_{k+1} = \mathbf{F}\boldsymbol{x}_k + \mathbf{L}f_k + \boldsymbol{q}_k \tag{56}$$

During the development of the equations shown in table II, we began with the discrete-time measurement and process models shown in (10) and (11). From there, state augmentation was used to model time correlation in the input noise distributions, culminating in (20) and (21). In the context of this example, (55) and (56) correspond to the models shown in (20) and (21) and (48) corresponds to (10). What is missing then is an equation corresponding to (11). To obtain this equation, we must integrate (46) and (47).

Integrating (47) over one accelerometer sampling interval results in

$$u_{k+1} = u_k + \int_{t_k}^{t_{k+1}} [f(\tau) + w(\tau)]\, d\tau \tag{57}$$

The measurement output from the accelerometer is precisely the integral on the right hand side of (57). Therefore

$$u_{k+1} = u_k + \Delta\upsilon_k + w_k \tag{58}$$

where $\Delta\upsilon_k$ is the accelerometer "delta v" measurement with an associated error of w_k.

Assuming that the acceleration of the vehicle is constant over one accelerometer sampling interval, we know from elementary physics that the position of the vehicle can be updated according to the equation

$$x_{k+1} = x_k + u_k \Delta t_a + \frac{1}{2} f_k \Delta t_a^2 \tag{59}$$

where Δt_a is the accelerometer sampling interval.

Noting that $f_k \Delta t_a = \Delta\upsilon_k + w_k$, (59) can be expressed as

$$x_{k+1} = x_k + u_k \Delta t_a + \frac{1}{2}\Delta t_a \Delta\upsilon_k + \frac{1}{2}\Delta t_a\, w_k \tag{60}$$

Equations (58) and (60) constitute the discrete-time dynamic model corresponding to (11).

$$\begin{bmatrix}x_{k+1}\\ u_{k+1}\end{bmatrix} = \begin{bmatrix}1 & \Delta t_a\\ 0 & 1\end{bmatrix}\begin{bmatrix}x_k\\ u_k\end{bmatrix} + \begin{bmatrix}\frac{1}{2}\Delta t_a\\ 1\end{bmatrix}\Delta\upsilon_k + \begin{bmatrix}\frac{1}{2}\Delta t_a\\ 1\end{bmatrix} w_k \tag{61}$$

The simulation parameters are as follows

TABLE III. NOMINAL FILTER PARAMETERS

Parameter	Value Used in Simulation
Range measurement sampling interval	Δt_b = 1.0 s
Accelerometer sampling interval	Δt_a = 0.5 s
Accelerometer white noise (√PSD)	10 μg/sqrt(Hz)
Accelerometer bias (1σ)	50 μg
Accelerometer bias time constant	τ_a = 75 s
Range measurement white noise (1σ)	0.3 m
Range measurement bias (1σ)	0.4 m
Range measurement bias time constant	τ_b = 60 s

The bounding curves are exponential functions with the following variances and time constants.

TABLE IV. DEFINITION OF BOUNDING FUNCTIONS

Parameter	Value Used in Simulation
Ranging measurement lower bound	$r_{0,l}$ = 0.1 m^2 , $\tau_{m,l}$ = 40 sec
Ranging measurement upper	$r_{0,u}$ = 0.3 m^2 , $\tau_{m,u}$ = 80 sec

Parameter	Value Used in Simulation
bound	
Accelerometer lower bound	$r_{0,l} = (20\ \mu g)^2$, $\tau_{a,l} = 50$ sec
Accelerometer upper bound	$r_{0,u} = (30\ \mu g)^2$, $\tau_{a,u} = 100$ sec

Using the simulation parameters shown in tables III and IV, we get the following results

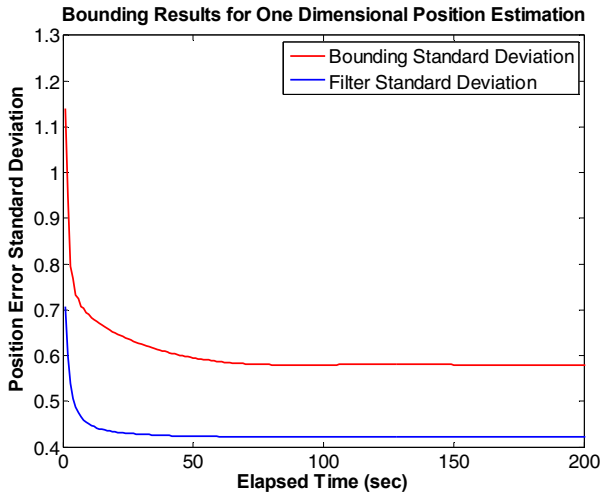

1–D position and velocity estimation

It is clear from figure 3 that the bounding algorithm provides an upper bound on the true estimate error standard deviation. This simulation provides numerical validation that the methods described in this work can be used to provide upper bounds on integrity risk. In future work, these methods will be applied to more practical applications involving measurements from multiple satellites and from three-dimensional triads of inertial measurement sensors.

CONCLUSION

In this work, we provided a method to upper bound the integrity risk associated with recursive estimators. Using the Kalman filter in particular, it was shown that the estimate error difference equation can be solved using the impulse response. Formulating the solution in this fashion allows existing methods developed for batch estimators to applied here. Using a one-dimensional position and velocity estimation problem as an example, it was shown that the variance output from the bounding algorithm does indeed upper bound the true estimate error variance. These algorithms provide an efficient approach to ensuring integrity in the presence of structured time correlation modeling uncertainty.

ACKNOWLEDGEMENTS

We would like to gratefully acknowledge our research sponsors at Navair and L3 Communications. Without their continued support, this research would not have been possible.

REFERENCES

[1] B. DeCleene, *Defining Pseudorange Integrity-Overbounding*, Proceedings of the Institute of Navigation's ION-GPS 2000, pp. 1916 – 1924.

[2] J. Rife, S. Pullen, B. Pervan, and P. Enge, *Paired Overbounding and Application to GPS Augmentation*, IEEE Position, Location and Navigation Symposium, pp. 439-446, 2004.

[3] J. Rife and D. Gebre-Egziabher, *Symmetric Overbounding of Correlated Errors*, NAVIGATION, 2007, Vol. 54, No. 2, pp. 109-124.

[4] G.W. Pulford, *A Proof of the Spherically Symmetric Overbounding Theorem for Linear Systems*, NAVIGATION, 2008, Vol. 55, No. 4, pp. 283-292.

[5] S. Khanafseh, S. Langel and B. Pervan, *Overbounding Position Errors in the Presence of Carrier Phase Multipath Error Model Uncertainty*, IEEE/ION Position, Location and Navigation Symposium, 2010, pp. 575-584.

[6] S.Langel, S.Khanafseh and B. Pervan, *Bounding Integrity Risk in the Presence of Parametric Time Correlation Uncertainty*, ITM 2012.

[7] Gelb, Arthur. Applied Optimal Estimation. The Analytic Sciences Corporation, 1974.

[8] Hwang, Patrick Y. and Robert Grover Brown. Introduction to RandomSignals and Applied Kalman Filtering. John Wiley and Sons, Inc. 1997.

[9] Schneider, Hans. Matrices and Linear Algebra New York: Holt, Rinehart and Winston, Inc., 1968.